Spectral statistics in chiral-orthogonal disordered systems

2003 J. Phys. A: Math. Gen. 36 3237

(http://iopscience.iop.org/0305-4470/36/12/322)

INSTITUTE OF PHYSICS PUBLISHING JOURNAL OF PHYSICS A: MATHEMATICAL AND GENERAL

J. Phys. A: Math. Gen. **36** (2003) 3237–3254 PII: S0305-4470(03)38068-0

Spectral statistics in chiral-orthogonal disordered systems

S N Evangelou[1,2] **and D E Katsanos**[1]

[1] Department of Physics, University of Ioannina, Ioannina 45110, Greece
[2] Department of Physics, University of Lancaster, Lancaster SW1 2BZ, UK

E-mail: sevagel@cc.uoi.gr

Received 12 June 2002, in final form 6 November 2002
Published 12 March 2003
Online at stacks.iop.org/JPhysA/36/3237

Abstract

We describe the singularities in the averaged density of states and the corresponding statistics of the energy levels in two- (2D) and three-dimensional (3D) chiral symmetric and time-reversal invariant disordered systems, realized in bipartite lattices with real off-diagonal disorder. For off-diagonal disorder of zero mean, we obtain a singular density of states in 2D which becomes much less pronounced in 3D, while the level-statistics can be described by a semi-Poisson distribution with mostly critical fractal states in 2D and Wigner surmise with mostly delocalized states in 3D. For logarithmic off-diagonal disorder of large strength, we find behaviour indistinguishable from ordinary disorder with strong localization in any dimension but in addition one-dimensional $1/|E|$ Dyson-like asymptotic spectral singularities. The off-diagonal disorder is also shown to enhance the propagation of two interacting particles similarly to systems with diagonal disorder. Although disordered models with chiral symmetry differ from non-chiral ones due to the presence of spectral singularities, both share the same qualitative localization properties except at the chiral symmetry point $E = 0$ which is critical.

PACS numbers: 05.45.Df, 72.15.Rn, 11.30.Rd

1. Introduction

In the last couple of decades the effect of various symmetries in the scaling theory [1] of Anderson localization has been explored, both theoretically and experimentally, leading to fundamental results [2]. For example, in two-dimensional (2D) disordered systems, breaking of the symmetry under time reversal leads to the quantum Hall effect where the presence of a magnetic field is responsible for critical delocalized states at the centre of each Landau band which carries the Hall current [3], while breaking of symmetry under spin-rotation due to

spin–orbit coupling is believed to lead to a metallic phase even in 2D [4]. Recently, much interest has focused on other basic symmetries, such as the chiral or particle–hole symmetry. In addition to the three standard universality classes (orthogonal, unitary and symplectic), the presence of chiral symmetry gives three extra chiral ensembles [5, 6], while four similar but distinct ensembles are realized for particle–hole symmetry in normal metal–superconducting systems, increasing their total number to 10 [7]. The prerequisite for chiral symmetry is the presence of bipartite lattice structure with two interconnected sublattices and the simplest case where it can be realized in disordered systems is real random hopping between nearest neighbours [8]. This is also known as off-diagonal disorder and it is worth studying the spectral and localization properties of such systems in order to see the effect of chirality in 2D and 3D. The presence of chiral symmetry in disordered systems somehow simplifies both analytical and numerical calculations so that more is known about Anderson localization for the chiral symmetry classes in one, quasi-one and two dimensions, illustrated for quasi-one dimension in [9]. In the rest of the paper we will rely on numerical tools in order to explore quantities that have not been computed analytically so far and also for quantities where the analytical predictions are competing, such as the 2D density of states.

The chiral symmetry is present in simple nearest-neighbour models with off-diagonal disorder defined on bipartite lattices which consist of two sublattices A and B, one connected to the other by random bonds [8]. This geometric kind of symmetry, where the randomness strictly connects sites of two different sublattices, is different from other intrinsic symmetries of the Hamiltonian such as time reversal and spin-rotation. It can also appear as an electron–hole transformation in half-filled many-body systems [7, 10]. It is well known that a consequence of the chiral symmetry is a distinct special point in the energy spectrum, for off-diagonal disorder in square and cubic lattices this is the band centre $E = 0$ with the eigenvalues making up symmetric energy pairs $(E, -E)$ around the zero mode $E = 0$. For an early observation of localized chiral zero modes see [11]. For finite lattices the special chiral energy eigenvalue $E = 0$ exists for any disorder configuration but only when the total number of sites is odd. Moreover, the corresponding $E = 0$ wavefunction is non-zero in one sublattice only and can be easily constructed [12, 13]. In fact, for any bipartite lattice with off-diagonal disorder only and n_A ($n_B \leqslant n_A$) sites belonging to sublattice A (B) the number of linearly independent $E = 0$ states is exactly $n_A - n_B$, with their amplitudes being non-zero on the A sublattice and exactly zero on the B sublattice. The chiral $E = 0$ state turns out to be neither localized nor extended but critical in all dimensions, also being very sensitive to the choice of boundary conditions [14], reminiscent of critical states at the mobility edge of the Anderson transition [15]. The main issue discussed in this paper is the singular behaviour of the density of states in 2D and 3D, when approaching the special chiral symmetry energy $E = 0$ where the localization length also diverges [8, 16].

The interest in this problem has been recently revived, due to the related problem of massless Dirac fermions in random gauge fields in [17][3] followed by [18–20] and also the Bogoliubov–de Gennes (BdG) Hamiltonians [21] which describe superconducting quasiparticles in mean-field theory. The Dirac fermions have very different zero disorder limit from the off-diagonal disorder case. In tight-binding approximation the 2D fermions have a zero energy Fermi surface with many points forming a square while the Dirac fermions have a Fermi surface with four points only. In the former case the pure 2D density of states at $E = 0$ has the well-known log-type van Hove singularity while in the Dirac case the density of states approaches zero at the band centre [21].

[3] Verbaarschot and Zahed have introduced in the zero-dimensional limit random matrix models with real eigenvalues to describe local fluctuations of the Dirac operator at the origin.

First, let us summarize what is known about the spectral and wavefunction anomalies of one-electron spectra in the presence of off-diagonal disorder in bipartite lattices described by real symmetric random Hamiltonians. The 1D random hopping problem in a bipartite lattice has a chiral spectrum with a strong $1/|E\ln^3|E||$ leading Dyson singularity of the density of states as E approaches zero, which is the first result obtained in disordered systems [22], even before the Anderson theory of localization was proposed [23]. The corresponding states of the energy spectrum are Anderson localized with their wavefunction amplitude decaying exponentially as $|\psi_{E\neq 0}(r)| \sim \mathrm{e}^{-\gamma r}$, where r is the distance and γ is the inverse localization length which depends on the disorder. This is not true at the chiral symmetry zero mode $E = 0$, where the corresponding wavefunction amplitude which lies in one sublattice decays slower than exponential, as $|\psi_{E=0}(r)| \sim \mathrm{e}^{-\gamma\sqrt{r}}$ at a distance r from its maximum where γ also varies with disorder. This result for the typical $E = 0$ wavefunction can be easily derived since its log-amplitude $\ln|\psi_{E=0}(r)|$ at site r executes a random-walk in space [8] leading to the exponential square root decay. In higher-dimensional bipartite systems, such as the square 2D or cubic 3D lattices, the $E = 0$ wavefunction was shown to display multifractal fluctuations with many scattered peaks and a disorder-dependent fractal dimension [13]. Moreover, an appropriate correlation function behaves logarithmically which roughly implies an overall power-law decay $|\psi_{E=0}(r)| \sim r^{-\eta}$ of the peak heights from the maximum peak with disorder dependent-η. It must be understood that such a power-law description is only a simplified picture for an approximate decaying character of the $E = 0$ critical state. For chiral systems the density of states at the band centre does not diverge only in 1D. In the absence of time-reversal symmetry on a 2D bipartite lattice for weak disorder in the vicinity of the band centre, the divergence $\rho_{2\mathrm{D}}(E) \sim |E|^{-1}\exp\left(-c\left(\ln\frac{1}{|E|}\right)^{\kappa}\right)$ was predicted by Gade [5] with a constant c and a universal exponent $\kappa = 1/2$. If universality applies, this singularity should also hold for the chiral-orthogonal ensemble. For strong disorder, Mortunich *et al* [24] argued that the exponent $\kappa = 1/2$ does not apply for a typical density of states in the chiral-orthogonal universality class and predict $\kappa = 2/3$ instead. In [25] the density of states for the π-flux phase is discussed via a weak disorder approach. The analytical work of [26] gives a wealth of exact results for the π-flux phase weakly perturbed by real nearest-neighbour hoppings. Recent work [27] for random Dirac fermions instead of vanishing density of states shows an upturn close to $E = 0$, in agreement with the diverging dos of Gade [5]. The multifractal analysis of [28] is compared to the analytical results of [20].

In this paper we shall investigate the consequences of the chiral symmetry for real symmetric random matrices in the orthogonal universality class by studying the spectrum of 2D and 3D square and cubic tight binding lattices with off-diagonal disorder. In the studied systems, apart from chirality, the symmetries of time reversal and spin-rotation are preserved as well. We shall determine the midband singularities in the density of states $\rho(E)$ and from the nearest-level-statistics the localization properties of the corresponding eigenstates. Our results demonstrate the effect of chirality for the unique off-diagonal disorder choice of mean zero: in 2D the nearest level-spacing distribution function $P(S)$ turns out to be intermediate between Wigner and Poisson roughly described by the so-called semi-Poisson curve [15] (for small spacings shows Wigner-like linear increase $\propto S$ and for large spacings shows a Poisson-like exponential decrease $\propto \exp(-S)$), which indicates the presence of critical states in finite 2D disordered systems. In 3D our results for the eigenvalue spacing fluctuations with zero mean off-diagonal disorder are very close to the Wigner surmise which corresponds to extended states. For logarithmic off-diagonal disorder which permits its strength to vary, we see for very strong values that the distributions in both 2D and 3D become Poisson-like independent of the dimension and the states localize similarly to those of ordinary disordered systems with broken chiral symmetry. Apart from clarifying the effect of chiral symmetry for

non-interacting electrons in disordered media, our aim is also to extend our calculations to more than one electron by including Hubbard electron–electron interactions together with off-diagonal disorder, via the simplest possible two-electron Hamiltonian. This is done in order to discuss a recent conjecture concerning the decisive role of chiral symmetry for quantum transport properties in the presence of both disorder and interactions at half-filling, where enhancement of the conductivity with increasing disorder was recently obtained only for non-chiral systems at half-filling [29][4].

We present a numerical study of the spectrum and its fluctuations in squared and cubic bipartite lattices with disorder in the nearest-neighbour hoppings. We summarize our main questions. (i) What is the nature of the spectral singularities in the presence of chiral symmetry? (ii) What is the corresponding level-statistics and the localization behaviour for disordered systems when chiral symmetry is preserved? (iii) From the established spectral and localization behaviour for systems with chiral or broken chiral symmetry, can we conclude whether all states remain localized in 2D? (iv) How is the electron–electron interaction affected by off-diagonal disorder for two particles only? Apart from the theoretical interest in answering the above questions, we emphasize that our study of localization with off-diagonal disorder can have many applications. In particular, the presence or absence of the chiral symmetry could be useful for understanding various properties of several realistic 2D systems, such as current-carrying states in the quantum Hall effect [3], quasiparticles in dirty superconductors [27], states in semiconductor quantum wells, high mobility silicon MOSFETs [30], etc.

2. The disordered Hamiltonian with chiral symmetry

We consider a tight-binding model Hamiltonian defined in bipartite lattices with random nearest-neighbour hoppings of the off-diagonal block symmetric structure

$$H = \sum_{\langle ij \rangle} \left(t_{ij} c_i^{\dagger} c_j + \text{H.c.} \right) = \begin{pmatrix} 0 & H_{A,B} \\ H_{A,B}^{+} & 0 \end{pmatrix} \tag{1}$$

where the sum is taken over all bonds $\langle ij \rangle$ where i, j denote nearest neighbour lattice sites which belong to different sublattices, c_i is the annihilation operator of an electron on site i and t_{ij} is the nearest-neighbour hopping integrals which are real independent random variables satisfying a box probability distribution with mean zero and arbitrary variance. This is equivalent to choosing random hoppings $t_{i,j}$ from a box distribution $P(t_{ij}) = \frac{1}{w}$, for $-\frac{w}{2} \leqslant t_{ij} \leqslant \frac{w}{2}$ of zero mean and width w. The scaling $t_{i,j}/w$ is sufficient to make the disorder independent of w, due to the absence of other energy scales in the Hamiltonian. Thus, by increasing w the energy band becomes wider since it amounts to a rigid rescaling of the eigenvalues only (the eigenstates remain the same for any w) and this is a unique form of *zero mean* off-diagonal disorder which allows certain comparison with analytical results to be made. The alternative choice is disorder of mean zero and width W but for the $\ln t_{i,j}$. This *logarithmic* disorder distribution is W-dependent, can be broad becoming arbitrarily strong and always guarantees positive hoppings $t_{i,j}$. It is commonly used in 1D where the real hoppings $t_{i,j}$ chosen from a logarithmic range must be always positive and can be widely varied with typical W, which is believed to be a good measure of off-diagonal disorder more generally. We emphasize that in our study the random distribution of the hoppings t_{ij} is the only disorder ingredient in the Hamiltonian H, since we completely ignore diagonal disorder by setting all site energies equal to zero. The diagonal disorder, somehow,

[4] Denteneer *et al* showed that the conductivity decreases with increasing disorder in half-filled chiral systems, the opposite to what occurs for non-chiral systems. This shows an unexpected tendency of the chirality to protect the insulating behaviour allowing the possibility of a metallic phase in 2D only for broken chiral symmetry.

connects each site to itself breaking the chiral symmetry. In our studies we consider finite $L \times L$ square and $L \times L \times L$ cubic lattices with various choices of boundary conditions, taking care to preserve the bipartite structure and chirality of H.

In equation (1) the matrix $H_{A,B}$ contains matrix elements which connect the A, B interconnected sublattices defining the two A, B bases, and due to chiral symmetry the Hamiltonian transforms as

$$H = -\sigma_3 H \sigma_3 \qquad \sigma_3 = \begin{pmatrix} 1 & 0 \\ 0 & -1 \end{pmatrix} \tag{2}$$

which means anticommuting H and σ_3. One notes that σ_3 behaves like the γ_5 familiar from applications of gauge theories [17]. Moreover, the presence of chiral symmetry allows one to reduce the size of the corresponding matrices to half by diagonalizing H^2 instead of H, obtaining the eigenvalues squared. Due to the interconnections by the random hoppings sublattice structure of the studied lattices [12] the eigenvalues appear in pairs $E, -E$ around $E = 0$ so that the spectral density is strictly an even function $\rho(E) = \rho(-E)$ of the energy E. The eigenvalue pairs $E, -E$ around $E = 0$ have simply related eigenstates $\psi_E(\vec{r}) = \sum_{n,l,\ldots} \psi_{n,l,\ldots} |n, l, \ldots\rangle$ and $\psi_{-E}(\vec{r}) = \sum_{n,l,\ldots} (-1)^{n+l+\cdots} \psi_{n,l,\ldots} |n, l, \ldots\rangle$ since $H\psi = E\psi$ from equation (2) gives $H\sigma_3\psi = -E\sigma_3\psi$ so that the unitary transformation σ_3 changes the wavefunction amplitude of the $-E$ state on every other site, say on the sites of sublattice B, keeping the amplitudes of the $-E$ state the same as that of E on sublattice A. Moreover, the $E = 0$ state when it exists (for odd total number of sites) has amplitude only on the A sublattice and is strictly zero on the B sublattice.

In order to measure the anomalies in the spectral density and their corresponding fluctuations, we obtained the eigenvalues of finite Hamiltonian matrices of size $L^d \times L^d$, $d = 2, 3$ for 2D and 3D, respectively. The very sparse matrices are obtained from equation (1) by distributing either $t_{i,j}$ uniquely or $\ln t_{i,j}$, with various strengths W to cover a wider range of off-diagonal disorder. We have used standard diagonalization algorithms, including Gaussian elimination for computing the integrated density of states (idos) by employing eigenvalue counting theorems at fixed E [31] and the Lanczos algorithm for computing eigenvalues within an energy range [32]. Moreover, we have considered all possible boundary conditions [15], such as periodic in all directions, periodic in one and hard wall in the other or hard wall in all directions, always preserving the chiral symmetry. It must also be noted that crucial even–odd size effects [9, 33] may arise in this problem, for example, with periodic boundary conditions the sites of the A sublattice are connected to those of the B sublattice preserving chirality only for even linear size L. For odd L, the periodic boundary conditions join sites which no longer belong to different sublattices and the chiral symmetry is broken. For hard wall boundary conditions no such even–odd effects arise. We should also remember that the zero mode $E = 0$ for chiral systems exists for odd sizes only. More details of the numerical methods can be found in [31, 32].

3. Zero mean off-diagonal disorder

3.1. The singularities in the dos

In one dimension we cannot have zero mean off-diagonal disorder due to the finite probability of finding a zero bond which breaks the chain. Outside one dimension for this kind of disorder, some rigorous results are known, such as the Gade [5] and Motrunich *et al* [24] singularities. Earlier approximate results were derived with a $\frac{1}{N}$-expansion [34][5] since the studied model is

[5] Oppermann and Wegner in $1/N$-expansion found a singular behaviour of the dos for a bipartite lattice near $E = 0$.

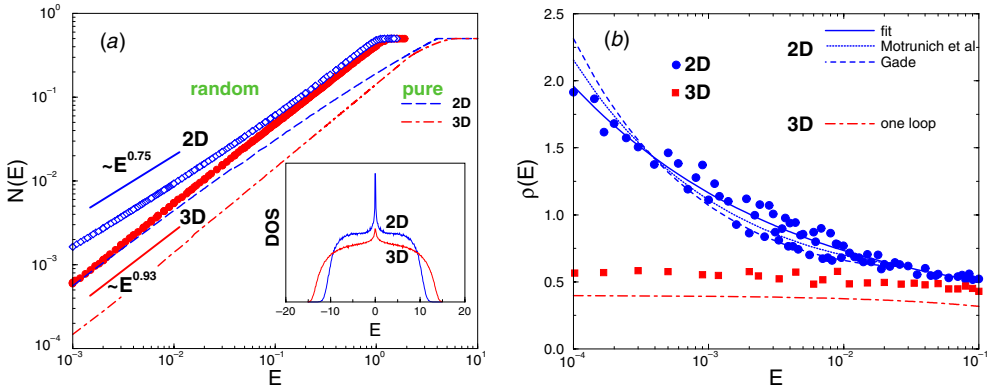

Figure 1. (*a*) Log–log plot of the 2D and 3D integrated density of states $\mathcal{N}(E)$, which measures the number of eigenvalues from 0 to E, with power-law fits of the numerical data for the zero mean off-diagonal disorder. The broken lines give the corresponding idos for the pure systems while the inset shows linear plots of the densities in the random case which display singularities at $E = 0$. (*b*) The 2D and 3D density of states $\rho(E)$ with the corresponding analytical forms of one loop [32], Gade [5] with $\kappa = 1/2$, Motrunich *et al* [24] with $\kappa = 2/3$ and our fit with $\kappa \approx 0.91$.

an example of the ensemble introduced in [10]. The extrapolation of the one-loop results near $E = 0$ [32] gives a logarithmic singularity in 2D dos

$$\rho_{2D}(E) = 0.299\,577\ldots + \frac{1}{2\pi^2}\ln\frac{1}{|E|} + O(|E|) \tag{3}$$

similar to that of the pure system where the constant term 0.299 577 is replaced by $\frac{1}{2\pi^2}\left(\ln 16 + \frac{1}{2}\ln 2\right) \approx 0.158\,0186$ [32, 34]. In the two-loop approximation the situation is less clear, for example, the corresponding term is divergent, proportional to $\left(\ln\frac{1}{|E|}\right)^2$, which might imply a power-law $\rho_{2D}(E) \propto |E|^{-\phi}$ spectral singularity. The small $|E|$ expression obtained in 2D by Gade [5] combines the strong $1/|E|$ divergence (Dyson-type) with a slowly decaying exponential of the logarithm of E to the power κ, written as their product

$$\rho_{2D}(E) = \frac{c_1}{|E|}\exp\left(-c_2\left(\ln\frac{1}{|E|}\right)^{\kappa}\right) \qquad \kappa = 1/2 \tag{4}$$

where c_1, c_2 are model-dependent constants. The improved strong disorder expression obtained by Motrunich *et al* [24] involves a different exponent for the logarithm $\kappa = 2/3$. In 3D the one-loop result gives a square-root singularity which remains for higher loops implying finite dos at $E = 0$ with

$$\rho_{3D}(E) = 0.400\,494\ldots - \frac{3\sqrt{3}}{2\pi^2}\sqrt{|E|} + O(|E|). \tag{5}$$

In figure 1 numerical results are presented for the averaged integrated dos (idos) $\mathcal{N}(E) = \int_0^E \mathrm{d}E'\rho(E')$ and the dos $\rho(E)$ close to $E = 0$. The random hoppings $t_{i,j}$ are uniformly distributed for example within $[-1/2, +1/2]$ since, of course, this specific range is irrelevant for localization. In order to determine the spectral singularities two possible fits are tried.

(i) A power-law fit for the idos $\mathcal{N}(E) \propto |E|^{1-\phi}$ which implies for the dos the power-law divergence $\rho(E) \propto |E|^{-\phi}$. In figure 1(*a*) numerical data for the idos $\mathcal{N}(E)$ which are obtained from eigenvalue-counting techniques allow one to compute the exponent ϕ for

squared and cubic lattice with lattice sizes up to 600×600 in 2D and $30 \times 30 \times 30$ in 3D. In the log–log plots the data are seen to collapse to power laws which define a small exponent $\phi \approx 0.25$ in 2D and $\phi \approx 0.07$ in 3D. These weak power-law divergences of the dos with off-diagonal disorder are certainly different from the expected log-type singularities of non-random systems in pure 2D and the constant dos in pure 3D (see figure 1).

(ii) We have also tried an alternative fit of the data in figure 1(*b*) by plotting directly $\rho(E)$ versus E in a semi-log plot. In 2D the data can be seen to be reasonably explained by the analytical form of Gade [5] and Motrunich *et al* [24]. The fit of Gade with $\kappa = 1/2$ gave $c_1 \approx 21.5, c_2 \approx 3.77$ and the fit of Motrunich *et al* with $\kappa = 2/3$ gave $c_1 \approx 2.61, c_2 \approx 2.14$. We have also tried another fit of the data which gave a slightly weaker power law in the exponential with the value $\kappa \approx 0.91$ and constants $c_1 \approx 0.47, c_2 \approx 1.04$. We also see that the one-loop result of equation (5) in 3D is clearly inappropriate to fit the small-$|E|$ data. Other fits can also be tried such as that of [35][6] which instead of $1/|E|$ from equation (4) involves the square root $1/\sqrt{|E|}$ leading divergence. The above fits (i) and (ii) verify that the presence of zero mean off-diagonal disorder leads to a weakly singular dos at least in 2D and a much weaker singularity, or a simple increase of the dos close to $E = 0$, in 3D.

3.2. The level-statistics

In order to check whether chirality has some effect on the localization properties, we proceed with the computation of spectral fluctuations via the nearest-level $P(S)$ distribution function. First we 'unfold' the spectrum by local rescaling of the energy scales to make the mean level spacing $\Delta(E) \propto 1/\rho(E)$ constant, equal to 1, throughout the spectrum. This is particularly important for a singular dos since the mean level spacing tends to zero at a singular point. Instead of the raw levels E_i, after 'unfolding' the spectrum consists of the 'unfolded' levels

$$\mathcal{E}_i = \mathcal{N}_{\rm av}(E_i) \qquad i = 1, 2, \ldots, N \tag{6}$$

obtained from the averaged integrated spectral density $\mathcal{N}_{\rm av}(E)$. For the 'unfolded' levels $\mathcal{E}_i$ the average nearest-level spacing becomes equal to 1. Moreover, for the localization properties of chiral systems, we should distinguish between the majority of levels in the spectrum $E \neq 0$ and the state at the chiral point $E = 0$.

In figure 2 we present the 2D nearest-level distribution function $P(S)$ obtained for zero mean off-diagonal disorder, various sizes L and boundary conditions (BC), using the majority of the energy levels in the band except those close to the band centre $E = 0$ and the tails. In 2D the results for various L seem to lie between the Wigner surmise (extended states) and the Poisson distribution (localized states), described by the intermediate semi-Poisson distribution $P(S) = 4S\exp(-2S)$ [15]. For small spacing $P(S)$ is Wigner-like and for large spacing the tails seen in the figure insets are Poisson-like. We have also performed averages of $P(S)$ over BC which can also be seen to be roughly described by the semi-Poisson curve [15]. It must be stressed that this distribution appears only for intermediate sizes with L smaller or close to the localization length ξ [16, 31, 35] in the considered energy window. The results obtained also agree with [36][7] where it is shown that the majority of the states for finite 2D disordered systems are multifractal for certain sizes L below ξ ($L \leqslant \xi$).

[6] The multifractal dimensions are expected to depend on the boundary conditions, even in the thermodynamic limit.

[7] Falko and Efetov have shown generic multifractality of localized 2D eigenstates with localization length ξ, as long as the size $L < \xi$ which corresponds to a diffusive system. This situation is usually met in 2D.

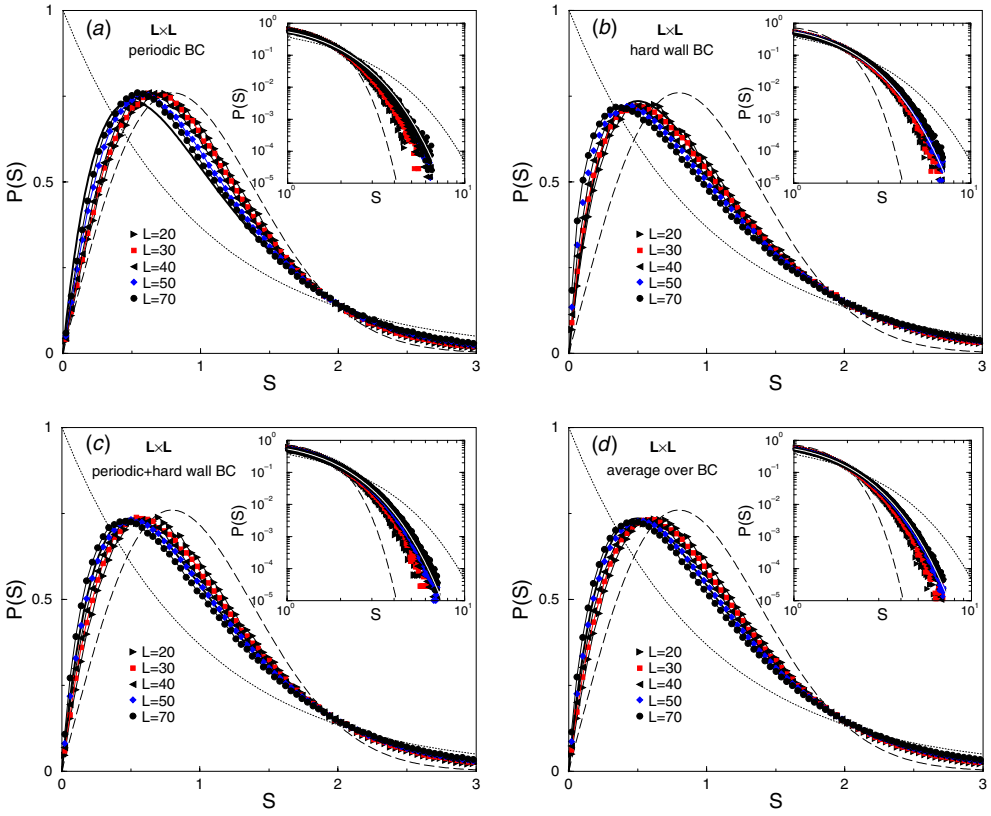

Figure 2. (a)–(d) The 2D nearest level-spacing distribution function $P(S)$ for zero mean off-diagonal disorder, various sizes L and three possible boundary conditions, such as periodic (PBC), hard wall (HWBC), periodic + hard wall and also the average over them. The dashed line is the Wigner surmise $P(S) = (\pi/2)S\exp(-(\pi/4)S^2)$, the dotted line is the Poisson law $P(S) = \exp(-S)$ and the solid line is the intermediate critical semi-Poisson distribution $P(S) = 4S\exp(-2S)$. In the insets we display log–log plots for the corresponding tails of $P(S)$. For $L = 20, 30, 40, 50, 70$ the number of runs is 5000, 6000, 10 000, 10 000, 3555, the eigenvalues were located in the energy band between [2, 6], for $w = 10$ where the full energy range is [0, 13], and their total number was a few million.

In order to demonstrate the effect of stronger level repulsion close to the chiral $E = 0$ state, we choose as an example a 1D chiral system with off-diagonal disorder for $L > \xi$ and an odd number of sites for the $E = 0$ state to exist. In figure 3 we plot the corresponding 1D spacing distribution $P(S)$ of the spacings S defined from the differences between the first from the zeroth $(E_1 - 0)$, the second from the first $(E_2 - E_1)$ and the eleventh from the tenth $(E_{11} - E_{10})$ eigenvalues for logarithmic disorder of $W = 1$. This involves 'unfolding' over the random statistical ensemble since the statistics of each spacing S is studied for many random configurations at fixed energy. We have additionally performed 'unfolding' over energy by using the well-known analytical form $\mathcal{N}_{\rm av}(E) = (W^2/9)/(\ln|E|)^2$ in 1D [8], working instead with the 'unfolded' levels $\mathcal{E}_i \propto 1/(\ln|E_i|)^2, i = 1, 2, \ldots, N$. We observe that the spacing distribution of the first positive eigenvalue from the zeroth shown in (a) is distinguished from the other spacing distributions (b) and (c) and clearly shows a higher degree of level repulsion. In this case the localization length ξ can also be obtained for every energy E from the expression $\xi(E) = (12/W^2)|\ln|E\|$ (e.g. see [8]). In figure 3 the considered size L is

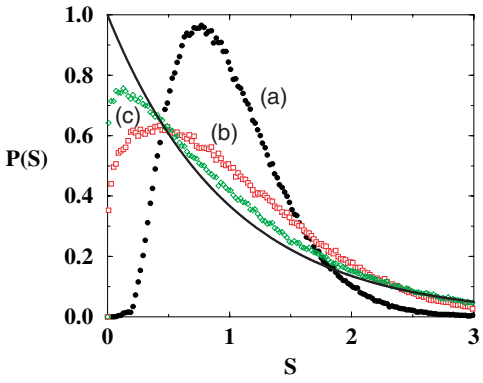

Figure 3. The 1D nearest level-spacing distribution function $P(S)$ of (a) the first from the zeroth (with localization length $\xi \approx 105$), (b) the second from the first ($\xi \approx 75$) and (c) the eleventh from the tenth ($\xi \approx 36$) eigenvalues for logarithmic off-diagonal disorder $W = 1$ and larger size $L = 1001$. The continuous line is the asymptotic Poisson law $P(S) = \exp(-S)$ valid for localized states in the limit $L \gg \xi$ and the total number of runs was 500 000. Note the double 'unfolding' performed over both disorder and energy since we are very close to the singular dos.

always larger than ξ but $P(S)$, which depends only on the ratio L/ξ, reaches the Poisson distribution only asymptotically, for L much larger than ξ. We emphasize again that for E close to the chiral energy $E = 0$ (where ξ is larger), the Poisson law for 1D localization is seen to be reached more slowly.

In figures 4(a) and (b) we return to the 2D zero mean case and plot the probability amplitude distribution of two typical multifractal wavefunctions at energies $E \neq 0$. They are seen to spread over space with fractal characteristics described by the fractal dimension D_2 and display many scattered peaks (scars). It must be pointed out for $E \neq 0$ the states are multifractal only for $L < \xi$ where ξ is their localization length, while the states at $E = 0$ where ξ diverges are described by multifractal dimensions valid for any size L [35]. In order to determine ξ instead of the exponential decay of the wavefunction amplitude on very long strips, alternatively we can count the number of sites where significant amplitude exists via the inverse participation ratio (IPR) [13, 35]. The computed IPR is a rough measure of ξ since it favours only the large amplitudes rather than the exponential tails of the amplitude distributions. The results for the average IPR in 2D are displayed versus energy E in figures 4(c) and (d) for various sizes L with hard wall and periodic BC, respectively. They allow one to estimate that localization is not yet reached for the studied energy region with the considered sizes L lower than or equal to the localization length ξ. For example, in figures 4(c) and (d) we can see that for the largest size $L = 100$ the mean IPR is close to convergence, which implies that ξ is roughly of the same order of magnitude ($\xi \approx L$). In figures 4(c) and (d) localization should be reached only when the curves of the mean IPR for two different sizes coincide. We can also speculate that the semi-Poisson appears because in the considered energy range for $P(S)$ in figure 2 we encounter a crossover situation where ξ, which does not vary much with E, obeys $L \lesssim \xi$, that is L is roughly smaller than or equal to ξ. The intermediate semi-Poisson distribution found in 2D, apart from being intimately connected to the underlying multifractality of the wavefunctions (for $L < \xi$), can be regarded as a crossover distribution with $L \approx \xi$. We emphasize that the adopted energy range lies in the middle between $E = 0$ and the tail with the chosen sizes L either smaller than or close to the wavefunction radius estimated by the corresponding ξ.

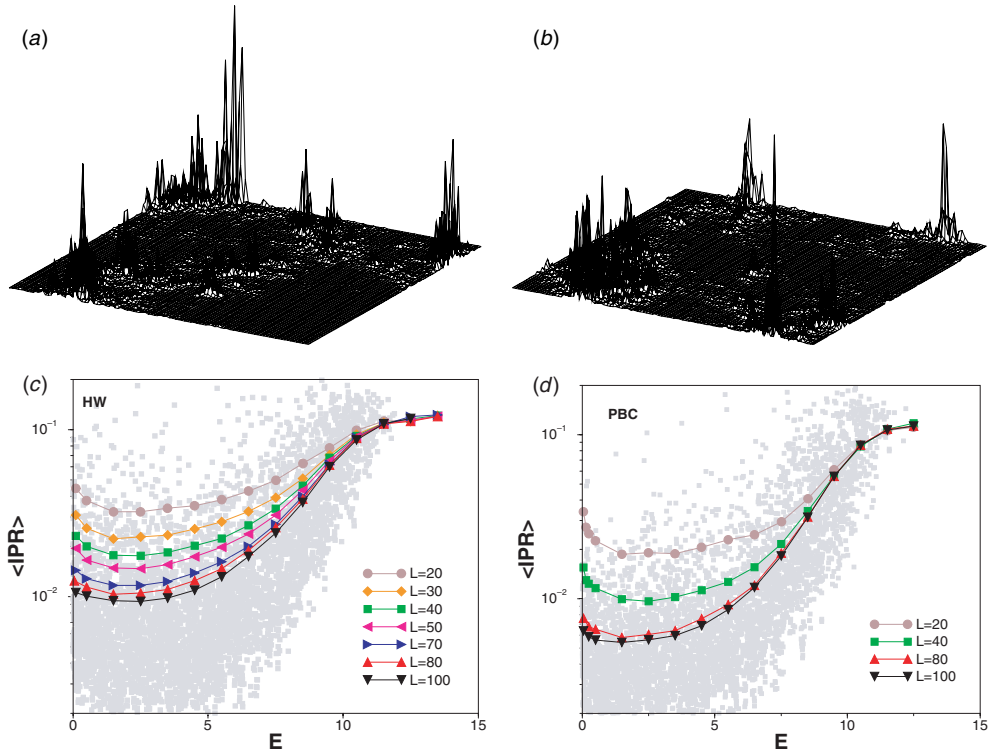

Figure 4. (*a*), (*b*) The amplitude distributions of two typical eigenstates for zero mean off-diagonal disorder in 2D away from the band centre $E \neq 0$. The states are multifractal only on scales below the localization length $L < \xi$ [36]. The behaviour of the $E = 0$ state when it exists is different since this state is critical for any size with fractal dimension D_2 ranging from the space dimension $D_2 = d$ for weak off-diagonal disorder to $D_2 = 0$ for strong off-diagonal disorder [13]. (*c*), (*d*) The corresponding average inverse participation ratio $\langle IPR \rangle$ versus energy E in 2D for various chiral even systems with hard wall and periodic BC, respectively. Note the values of $\langle IPR \rangle$ are lower for PBC where the states are slightly more extended in comparison. For finite systems from IPR $\propto L^{-D_2}$ near the minimum of the curves we find $D_2 \approx 0.8$, slightly higher D_2 near $E = 0$ and much lower D_2 (localized states) for large E. The absence of saturation of the curves implies that the adopted system sizes are smaller than the localization length ($L \lesssim \xi$). In the background with grey squares we see the actual values of IPR for the size $L = 100$ only. They display enormous fluctuations and are used for computing the corresponding average for $L = 100$.

The semi-Poisson $P(S)$ distribution obtained and the multifractality for finite size in 2D concern states only within the band ($E \neq 0$) for finite $L \lesssim \xi$. For the zero mean off-diagonal disorder, the chosen sizes L are smaller than or equal to the localization length ξ. However, for larger $L \gg \xi$ (we cannot reach such L in our 2D calculations) the data from figure 2 should eventually approach the Poisson curve which indicates only localized states in 2D. The very slow approach to the localized Poisson limit for infinite size $L \to \infty$ is expected here except at the band centre $E = 0$ where ξ also diverges [16, 35]. In 3D the $P(S)$ obtained for this zero mean off-diagonal disorder is shown in figure 5 to lie very close to the Wigner surmise, a result compatible with the existence of mostly delocalized states in 3D. This implies an asymptotic approach towards Wigner for this kind of off-diagonal disorder. In other words, the obtained behaviour exhibited by $P(S)$ for $E \neq 0$ suggests critical behaviour only for finite systems in 2D and delocalized diffusive behaviour for any size in 3D. Therefore, the localization properties of chiral systems outside the chiral

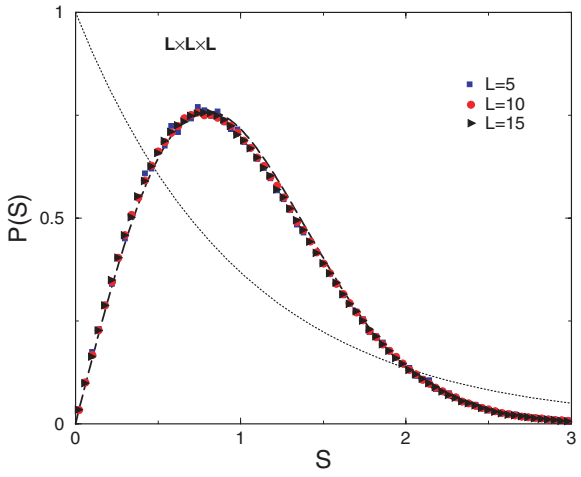

Figure 5. The 3D nearest level-spacing distribution function $P(S)$ for the zero mean off-diagonal disorder, various system sizes L with the dashed line giving the Wigner surmise $P(S) = (\pi/2)S\exp(-(\pi/4)S^2)$. The sizes $L = 5, 10, 15$ shown are diagonalized for 5000, 6000, 2000 configurations and a total number of a few million eigenvalues were considered in each case.

energy $E = 0$ in any dimension are similar to those of ordinary disordered systems with the corresponding localization length ξ.

We have also checked the probability distributions for the first few eigenvalues close to $E = 0$ by employing many random configurations (realizations of disorder) as done in [35]. This demonstrates nicely the level repulsion (not shown) by using data for lattices of even numbers of sites with periodic BC and odd numbers of sites with hard wall BC, which preserve chiral symmetry. Although chirality is present in both cases the $E = 0$ state exists only for the latter odd case. We have observed the increase of the eigenvalue density $\rho(E)$ close to $E = 0$ for both even and odd sizes but could not draw any conclusions for the statistical behaviour of the energy levels since energy level repulsion can be examined only after 'unfolding'. For the even size L systems the two eigenvalues closest to $E = 0$ (the lowest positive one and the one with exactly the same energy but minus sign) always show level repulsion due to chiral symmetry. The level repulsion between the two energies E_1, $-E_1$ for the smallest possible E_1 is expected since these energies are always separated by the chiral symmetry point $E = 0$. On the other hand, the effect of level repulsion should also be enhanced for states close to $E = 0$ where the localization length ξ diverges (longer ξ implies stronger level repulsion). For odd size L with chiral symmetry the $E = 0$ eigenvalue exists for every random configuration. The conclusion which can be drawn from this paper is that scaling of level-statistics for $E \neq 0$ chiral systems is determined by the ratio of the system size L over the corresponding localization length ξ, similar to what happens for ordinary disordered systems, and a critical state exists at $E = 0$.

4. Logarithmic off-diagonal disorder

4.1. The $1/|E|$ *leading singularity*

In 2D the states away from the band centre ($E \neq 0$) are also weakly multifractal on scales below the localization length. The discontinuous behaviour claimed for the fractal dimension D_2 at the band centre in [35] is probably due to the different boundary conditions used for the

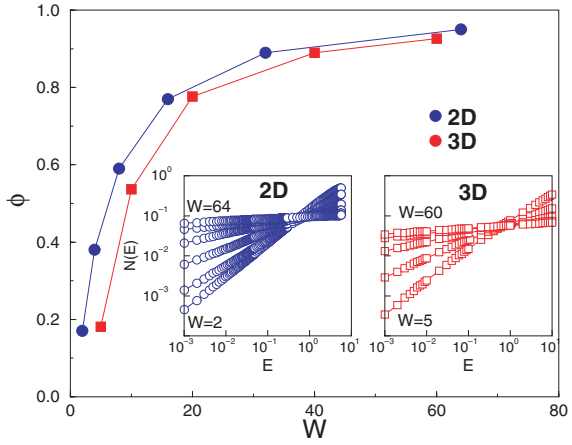

Figure 6. The exponent ϕ for the power-law fit of the density of state $\rho(E) \propto |E|^{-\phi}$ is shown in 2D and 3D to approach the 1D Dyson singularity limit (power law with $\phi = 1$). In the inset the corresponding idos for various values of the strength of logarithmic off-diagonal disorder are shown. Eigenvalue counting algorithms are used for sizes $L = 200, 400$ and $L = 30$ in 2D and 3D, respectively.

$E = 0$ and $E \neq 0$ states. At $E = 0$ where the localization length diverges, the corresponding state is multifractal for every length scale with a fractal dimension D_2 dependent on the strength of the logarithmic off-diagonal disorder W, ranging from 2 to 0 for very weak and very strong off-diagonal disorder, respectively. For strong off-diagonal disorder of width W for $\ln t_{i,j}$, the observed accumulation of levels close to $E = 0$ behaves differently. The data shown in figure 6 for 2D and 3D can be fitted to power-law singularities for the idos

$$\mathcal{N}(E) \propto |E|^{1-\phi} \Leftrightarrow \rho(E) \propto |E|^{-\phi} \tag{7}$$

with the exponent equal to ϕ. The $\mathcal{N}(E)$ and the fitted exponents ϕ are shown in figure 6 where the $1/|E|$ Dyson singularity which implies $\phi = 1$ is approached when W increases. This indicates that the behaviour depends on the strength W so that for a very strongly disordered medium, the density of states should approach its 1D Dyson limit, as predicted in [37]. This is also in agreement with the forms of Gade and Motrunich *et al*, forms having very small constant c_2 in equation (4).

4.2. The tridiagonalization method

The defined chiral 2D or 3D Hamiltonian H can be mapped onto a one-dimensional semi-infinite chain via the so-called tridiagonalization scheme [31, 37]. The spectral singularities and the degree of localization are then reflected in the statistical properties of the tridiagonal matrix created . This is a version of the Lanczos algorithm [38] which is normally a procedure for finding eigenvalues and eigenvectors of large sparse matrices with most matrix elements zero. The Lanczos method, like any other diagonalization method, reduces the matrix to a tridiagonal form proceeding as follows: one starts with a normalized starting state Φ_1 (e.g. corresponding to a central lattice site) and by operating successively with H generates the orthonormalized states Φ_n, via the recursion formula

$$\beta_n \Phi_n = (H - \alpha_{n-1})\Phi_{n-1} - \beta_{n-1}\Phi_{n-2} \tag{8}$$

$n = 2, \ldots, N$ and $\beta_1 = 0$. The new states $\Phi_n, n = 2, \ldots, N$ are linear combinations of the original lattice basis set, e.g. in 2D this set consists of the normalized states

$|n_1, n_2\rangle, n_1, n_2 = 0, \pm1, \pm2, \pm3, \ldots$. In the new $\Phi_1, \Phi_2, \ldots$ basis H is represented by a semi-infinite tridiagonal matrix where the diagonal matrix elements are $\alpha_n, n = 1, 2, \ldots, N$ and the off-diagonal $\beta_n, n = 2, 3, \ldots, N$. The tridiagonalization preserves chiral symmetry so that $\alpha_n = 0, n = 1, 2, \ldots, N$ for chiral systems. In this case if we start from the central site corresponding to the normalized state $\Phi_1 = |0, 0\rangle$ from equation (8) with zero α_n, we have $\Phi_2 = H\Phi_1/\beta_2, \Phi_3 = H\Phi_2/\beta_3 - (\beta_2/\beta_3)\Phi_1$, etc and the $\beta_n, n = 2, 3, \ldots$ are obtained at each step by normalizing the states $\Phi_2, \Phi_3, \ldots$. Since H is a nearest-neighbour Hamiltonian acting on $|n_1, n_2\rangle$, we can arrange the lattice into 'shells'. The state Φ_{n+1} includes all the lattice sites up to nth 'shell' (for zero disorder only the sites of the nth 'shell') which in 2D consist of the lattice sites $n_1, n_2 = 0, \pm1, \pm2, \pm3, \ldots$ so that $n = |n_1| + |n_2|$, starting from $\Phi_1 = |0, 0\rangle$. As an example, for the periodic 2D Hamiltonian one computes $\beta_2 = 2, \beta_3 = \sqrt{5}, \beta_4 = \sqrt{76/20}$, etc, approaching $\beta_{n\to\infty} = 2$. The basis states for the corresponding tridiagonal matrix are $\Phi_1 = |0, 0\rangle, \Phi_2 = (|1, 0\rangle + |0, 1\rangle + |-1, 0\rangle + |0, -1\rangle)/\beta_2$, $\Phi_3 = (|2, 0\rangle + |0, 2\rangle + |-2, 0\rangle + |0, -2\rangle + 2|1, 1\rangle + 2|1, -1\rangle + 2|-1, 1\rangle + 2|-1, -1\rangle)/(\beta_2\beta_3)$, etc.

The advantage of the tridiagonalization method is economy of storage since we can save only the α and β as we go along. The weakness of the method is loss of orthogonality due to rounding errors (although for sparse matrices the damage is smaller). In 2D or 3D if we start from a central site the matrix consists of blocks around it so that each block corresponds to a 'shell'. A site which can be reached from the central site (0th 'shell') in a minimum of n steps from the origin is in the 'shell' n. The 2D or 3D matrix is block-tridiagonal with blocks corresponding to 'shells' starting from the 0th 'shell' with Φ_1 and we can work with N iterations, exactly equal to the number of 'shells', to determine $\Phi_2, \Phi_3, \ldots, \Phi_{N+1}$ and $\beta_2, \beta_3, \ldots, \beta_{N+1}$ for the $1, 2, \ldots, N$th 'shells' around the central site. From the 1D semi-infinite tridiagonal matrix obtained, one can conveniently compute the local density of states on the central site Φ_1 which has its first $2N$ moments exactly equal to the spectral density of the original 2D or 3D matrix. It must be stressed that the use of the Lanczos algorithm nowadays is different from that of the tridiagonalization method. Its wide use is directed, instead, towards the computation of specific eigenvalues of large sparse matrices with the requested accuracy. This can be achieved by increasing the number of iterations to much larger values than the number of 'shells' or 'blocks' considered in tridiagonalization.

For zero disorder or disorder which preserves chiral symmetry connecting the A and B sublattices, a 2D or 3D tight-binding system maps to a chain with all $\alpha_n = 0$. For chiral disorder the mapping onto a 1D chain involves only off-diagonal disorder but inhomogeneous type (n-dependent) [37, 31]. It is only for very strong off-diagonal disorder where the disordered chain resulting from the tridiagonalization becomes homogeneously off-diagonal disordered. On the basis of our numerical results, we argue that although this conjecture holds, the suggested inhomogeneous decay in the case of not-so-strong disorder is absent as well (or it is not of power-law type).

Since for chiral systems the 1D semi-infinite chain is also chiral with off-diagonal disorder, only the well-known 1D results could map to higher dimensions. The resulting 1D chain from the tridiagonalization scheme has inhomogeneous off-diagonal disorder with hopping matrix elements β_n chosen from a site n-dependent random distribution of mean $\langle\beta_n\rangle$ and variance $\mathrm{var}(\beta_n) = \langle\beta_n^2\rangle - \langle\beta_n\rangle^2$. Under the approximation that the states Φ_{n+1} are expressed as linear combinations of $|n_1, n_2\rangle$ belonging to the nth 'shell' only, which is valid for pure systems and claimed to hold for weak off-diagonal disorder, in [37] a power-law decay of the variance versus n was predicted. This gave $\psi(r) \propto \mathrm{e}^{-\gamma\sqrt{\ln r}}$ decay of the $E = 0$ chiral state in every dimension higher than 1. Our numerics show that some of the arguments which led to this

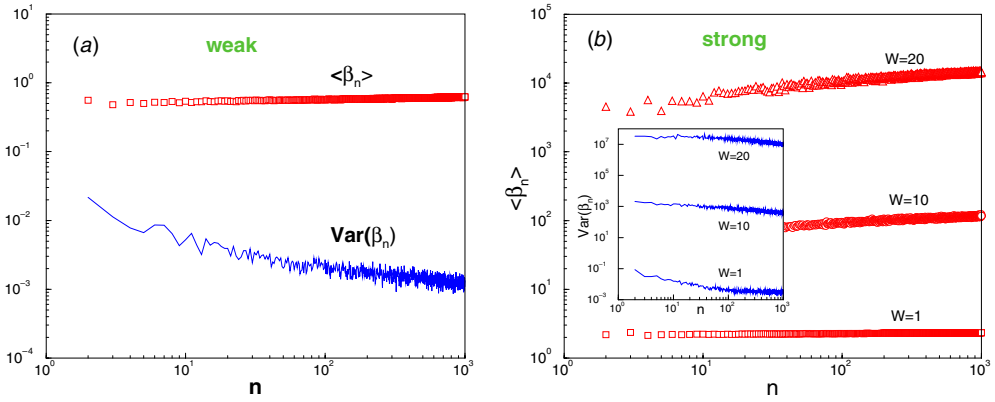

Figure 7. (*a*) The parameters of the tridiagonal chain with mean $\langle\beta_n\rangle$ and variance var(β_n) as a function of the chain index n for zero mean off-diagonal disorder and 5000 random configurations (2D). Although decay of the variance is seen for small n, implying inhomogeneous disorder for the chain, the data point towards saturation at large n. (*b*) The parameters of the tridiagonal chain $\langle\beta_n\rangle$ and their variance var(β_n) as a function of the tridiagonal chain index n for various values W of logarithmic off-diagonal disorder (2D). The saturation of the variance var(β_n) suggests a mapping of higher-dimensional strongly off-diagonal disordered systems to a random chain.

result are not valid since for weak off-diagonal disorder the variance versus n does not decay as a power law, but one eventually obtains indications of saturation for large n (although the data for smaller n could be fitted to power laws). For strong off-diagonal disorder the saturation obtained implies a constant var(β_n) independent of n and only in this case do the results for 1D off-diagonal disorder, such as the $1/|E|$ Dyson-type spectral singularities, carry through to higher dimensions.

In order to check these predictions we are able to extend the previous numerical calculations to a higher number of 'shells' n starting from a central site Φ_1 (0th 'shell'). For example, for the zero mean disorder in 2D we can go up to $N = 1000$ 'shells' starting from the site at the origin, and the total number of sites from the starting central site (0th 'shell') up to the Nth 'shell' is $2N^2 + 2N + 1$. For the largest N used we always find saturation of the variance versus n, even for the zero mean off-diagonal disorder (figure 7(*a*)) and certainly for the logarithmically strong off-diagonal disorder (figure 7(*b*)). The predicted inhomogeneous power-law decay of [37], which implies n-dependent variance, does not seem to hold but such a decay might exist only for finite sizes (small n). For large enough n for both zero mean and strong logarithmic off-diagonal disorder, the mapping to the 1D chain involves n-independent (homogeneous) disorder. The above discussion is not in favour of the square root of log exponential law predicted in the tridiagonalization of [37] and rather points towards the presence of $1/|E|$ forms for the dos in higher d predicted by Gade and Motrunich *et al*. For strong off-diagonal disorder the prediction of n-independent variance with associated 1D behaviour in 2D and 3D holds more clearly and the $1/|E|$ Dyson divergence should somehow appear. The data for the hoppings $\langle\beta_n\rangle$ and the variance var(β_n) versus n are shown in figure 7(*a*) for zero mean and figure 7(*b*) for strong logarithmic off-diagonal disorder. Although the saturation of $\langle\beta_n\rangle$ can be seen in all cases, the var(β_n) seems to decay for the zero mean off-diagonal disorder. However, this is true only for small n and the var(β_n) is eventually seen to have a tendency to saturate for larger n (figure 7(*a*)). For large W the saturation already occurs for smaller n (figure 7(*b*)). In 3D we have obtained similar results.

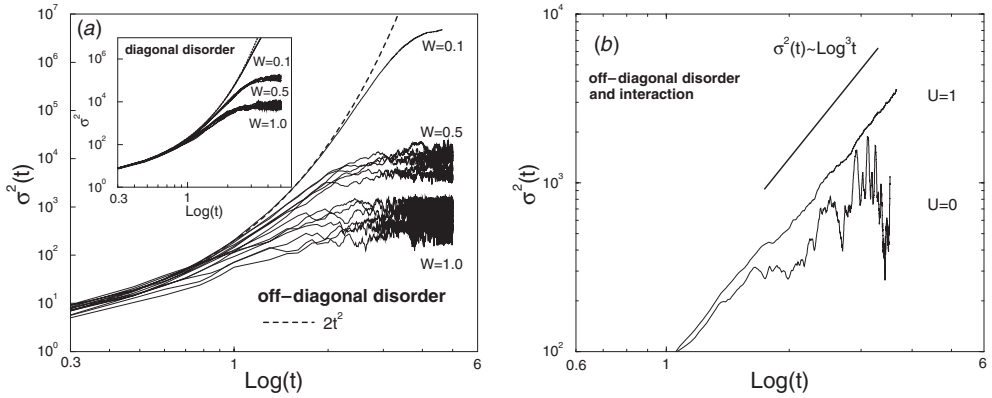

Figure 8. (*a*) Log–log plot of the mean-square displacement $\sigma^2(t)$ as a function of $\log(t)$ in 1D (note the double $\log(\log(t))$ in the x-axis so that 1, 6 correspond to $t = 10$, $t = 10^6$, respectively, and the single log σ^2 in the y-axis, all for base 10 logarithms) for logarithmic off-diagonal disorder with $W = 0.1$, $W = 0.5$ and $W = 1$. The dashed line is the ballistic limit $2t^2$. In the inset results for diagonal disorder from $[-W/2, +W/2]$ are shown. (*b*) A log–log plot of the mean-square displacement $\sigma^2(t)$ for two particles as a function of $\log(t)$ for logarithmic off-diagonal disorder with $W = 1$ and interaction strength $U = 0, 1$. The enhancement of the wavepacket propagation in the presence of interaction as well as the smoother evolution with an approximate ultraslow diffusive law can also be seen for off-diagonal disorder.

5. Dynamics of two interacting particles with off-diagonal disorder

In figure 8(*a*) we observe the dynamics of one particle for logarithmic off-diagonal disorder in 1D. We find that the effect of off-diagonal disorder turns out to be similar to that of diagonal disorder, both deviating from the pure chain ballistic law $\sigma^2(t) = 2t^2$ (dashed line in figure 8(*a*)) in proportion to the added disorder. Next we turn to the interacting case since the chiral symmetry (rather its absence) was recently shown to be crucial for the possibility of a metallic phase in 2D. For half-filled interacting systems, the Mott gap turns out to be insensitive to weak disorder when chiral symmetry is present, so that a metallic phase in 2D could become possible only when the chiral symmetry is broken [29].

In order to check the effect of repulsive interactions in the 1D chain, we have computed the mean square displacement from the formula

$$\sigma^2(t) = \tfrac{1}{2} \sum_{n_1,n_2} |\Psi_{n_1,n_2}(t)|^2 (n_1 - \overline{n}_1 + n_2 - \overline{n}_2)^2 \tag{9}$$

with $\Psi_{n_1,n_2}(t)$ being the time-dependent wavefunction for two particles at sites n_1, n_2 in the presence of off-diagonal disorder and interaction U [39, 40], both starting at the same initial zeroth site. The mean electron positions are $\overline{n}_i = \sum_{n_1,n_2} \left|\Psi_{n_1,n_2}(t)\right|^2 n_i$, $i = 1, 2$. The result for $\sigma^2(t)$ is shown in figure 8(*b*) for off-diagonal disorder without interaction ($U = 0$) and interaction of strength $U = 1$. We verify that the two-particle propagation increases with interaction, as for ordinary diagonal disorder where propagation is known to be enhanced in the presence of disorder when U is switched on [39, 40]. For increasing disorder we find that propagation decreases as expected. In the presence of both disorder and interaction, propagation is also seen to become smooth and the data obey an ultraslow diffusion law $\sigma^2(t) \propto \log^{\alpha}(t)$ with a slope from the linear fit $\alpha \approx 3$ (figure 8(*b*)) when $U = 1$. Unfortunately, we cannot discuss the half-filled chiral symmetric limit since our case involves only low filling of two particles. For $U \neq 0$ our system clearly violates the chiral symmetry since it is no longer

particle–hole symmetric due to U which is added in the matrix diagonal. More generally, a bipartite lattice structure with chiral symmetry was discussed in the absence of disorder [41] for general filling and dimension with interaction strength U. Their results hold for our chiral systems too since for negative U the spectrum turns out to be opposite to that for positive U while the energy E corresponds to the energy $-E$ of the other model. This implies that for certain initial conditions, the quantum evolution is the same for both positive and negative U [41].

6. Discussion

We have investigated numerically 2D and 3D models of non-interacting fermions and a 1D model of two interacting fermions, all cases with random nearest-neighbour hopping in bipartite systems. They belong to the chiral-orthogonal universality class where disorder respects chiral symmetry, manifesting itself in spectral singularities and certain anomalous localization behaviour at $E = 0$. It should be pointed out that the effect of chiral symmetry in disordered systems was suspected more than two decades ago in studies of off-diagonal disorder [8] and about a decade ago in similar studies of BdG Hamiltonians which describe dirty superconductors [42]. It was believed that exceptions to the scaling theory of localization might arise in these systems, such as spectral singularities and a kind of delocalization at the band centre in an otherwise localized spectrum. Moreover, depending on each author's viewpoint, the critical behaviour of the undoubtedly critical multifractal state at $E = 0$ was named either delocalization [19] or power-law localization [13], although both meant weakening of localization close to $E = 0$ where the localization length diverges. The $E = 0$ critical state can be fully described by multifractal exponents via scaling the amplitude moments, and its fractal dimensions, such as D_2, vary strongly with the strength of off-diagonal disorder ranging from space filling extended states $D_2 \to d$ for weak disorder to point-like localized states $D_2 \to 0$ for strong disorder. This transition in the multifractal spectrum is known as 'freezing transition' [20]. Below 'freezing' computed mean and typical values agree but not above 'freezing' where the means are determined by the tails of the corresponding distributions. In 3D for weak off-diagonal disorder where most states with $E \neq 0$ are extended, the critical $E = 0$ state also behaves as an extended state with $D_2 \approx d$. This picture also agrees with early transmission studies for particle–hole symmetric BdG Hamiltonians which showed that quasi-extended states may [42] or may not [43] exist, depending on the chosen energy E. The present work summarizes all effects of chiral symmetry such as spectral singularities in 2D for zero mean off-diagonal disorder which become strong $1/E$ Dyson-type singularities for strong off-diagonal disorder, while the corresponding level-statistics varies around the critical semi-Poisson curve for finite systems of size smaller than or equal to the localization length ($L \lesssim \xi$), suggesting that the $E \neq 0$ states from multifractal become fully localized for infinite size except for the chiral $E = 0$ energy state which is multifractal for any size, disorder and dimension [44, 45][8]. For strong off-diagonal disorder, we find that the behaviour for the rest of $E \neq 0$ states is indistinguishable from that of ordinary 2D disordered systems with the appropriate localization length.

The chiral symmetry realized in bipartite lattices when the disorder connects one sublattice to the other is characterized by enhanced dos and weakening of localization with a critical state at $E = 0$, having different spectral and localization properties from the $E \neq 0$ states. This answers questions (i) and (ii) set in the introduction. Concerning question (iii), 2D

[8] Fabrizio and Castellani have shown that the quantum correction to the conductivity in 2D vanishes at the band centre (the particle–hole symmetric point) implying delocalized states with a diverging dos. In 3D all states sufficiently close to the band centre $E = 0$ are extended. Our computations agree with their results.

delocalization in this context seems to require interacting electrons and possibly broken chiral symmetry [29]. About question (iv), the effect of chiral disorder on the electron–electron interaction for two particles seems to be no different from that of diagonal disorder. The main message of section 5 is that off-diagonal disorder has the same effect as diagonal disorder for coherent two interacting particle propagation, with the presence of ultraslow diffusion. Our study also offers answers to questions about the eigenstates. Outside the middle of the band ($E \neq 0$) criticality is expected to occur only for finite systems [36]. Instead, the $E = 0$ state is critical with fractal exponents close to space filling for small W (extended states) and point-like for large W (localized states) [40]. This is similar to what one expects for ordinary Anderson localized states with diagonal disorder.

In summary, we have presented numerical results for the density of states with off-diagonal disorder in order to test various theories which describe the observed spectral singularities, from *Dyson* to *Gade* and *Motrunich et al* forms. These results complement many analytical methods developed especially for unitary chiral systems. For *zero mean* off-diagonal disorder, our main finding is that the form of the spectral singularity in 2D is stronger than the log-type singularity of the pure system and can be fitted either with a weak power law or by the intermediate Gade or Motrunich *et al* forms and also their formula but with a new exponent κ. In 3D the dos is a little enhanced at $E = 0$ but when fitted to a power law the obtained divergence, if any, is very weak. The corresponding level-statistics for finite systems in 2D is close to the critical semi-Poisson curve and in 3D the Wigner curve, implying critical and extended states for the majority of states in the band for 2D and 3D, respectively. For logarithmically *strong* off-diagonal disorder, our results are indistinguishable from ordinary strongly disordered systems except at the midband critical state $E = 0$ where the chiral symmetry is responsible for anomalous delocalization. Emphasis is given in 2D where exceptions from generic localization are more pronounced in the form of large localization lengths and multifractality of all states for sizes below their localization length e.g. Poisson statistics in 2D. However, for large scales a chiral symmetric disordered system behaves like an ordinary disorder system with only two visible differences: (i) spectral singularities at the chiral energy $E = 0$ which become $1/|E|$ Dyson-like for strong disorder or low dimensionality and (ii) the presence of multifractality at the critical $E = 0$ symmetry point which becomes close to extended for zero mean disorder and localized for strong disorder. At other energies the chiral disorder has the same effect as ordinary disorder.

Acknowledgments

We would like to thank the referees for useful comments.

References

[1] Abrahams E *et al* 1979 *Phys. Rev. Lett.* **42** 673
[2] Hikami S *et al* 1980 *Prog. Theor. Phys.* **63** 707
[3] Huckestein B 1995 *Phys. Rep.* **67** 357
[4] Bergmann G 1984 *Phys. Rep.* **107** 1
[5] Gade R and Wegner F 1991 *Nucl. Phys.* B **360** 213
Gade R 1993 *Phys. Rev.* B **398** 499
[6] Slevin K and Nagao T 1993 *Phys. Rev. Lett.* **70** 635
[7] Altland A and Zirnbauer M R 1997 *Phys. Rev.* B **55** 1142
[8] Eggarter T P and Riedinger R 1978 *Phys. Rev.* B **18** 569
[9] Brouwer P W, Mudry C, Simons B D and Altland A 1998 *Phys. Rev. Lett.* **81** 862
Mudry C, Brouwer P W and Furusaki A 1999 *Phys. Rev.* B **59** 13221

Brouwer P W, Mudry C and Furusaki A 2000 *Phys. Rev. Lett.* **84** 2913
Brouwer P W, Mudry C and Furusaki A 2000 *Nucl. Phys.* B **565** 653
Mudry C, Brouwer P W and Furusaki A 2000 *Phys. Rev.* B **62** 8249
Titov M, Brouwer P W, Furusaki A and Mudry C 2001 *Phys. Rev.* B **63** 235318
[10] Wegner F J 1979 *Z. Phys.* B **35** 207
Wegner F J 1979 *Phys. Rev.* B **19** 783
[11] Sutherland B 1986 *Phys. Rev.* B **34** 5208
[12] Inui M, Trugman S A and Abrahams E 1994 *Phys. Rev.* B **49** 3190
[13] Xiong S J and Evangelou S N 2001 *Phys. Rev.* B **64** 113107
[14] Brouwer P W, Racine E, Furusaki A, Hatsugai Y, Morita Y and Mudry C 2002 *Phys. Rev.* B **66** 014204
[15] Braun D, Montambaux G and Pascaud M 1998 *Phys. Rev. Lett.* **81** 1062
[16] Eilmes A, Römer R A and Schreiber M 1998 *Eur. Phys. J.* **1** 29
[17] Verbaarschot J J M and Zahed I 1993 *Phys. Rev. Lett.* **70** 3852
Verbaarschot J J M and Zahed I 1994 *Phys. Rev. Lett.* **72** 2531
[18] Ludwig A W W, Fisher M P A, Shankar R and Grinstein G 1994 *Phys. Rev.* B **50** 7526
[19] Nersesyan A A, Tsvelik A M and Wenger F 1994 *Phys. Rev. Lett.* **72** 2628
Nersesyan A A, Tsvelik A M and Wenger F 1995 *Nucl. Phys.* B **438** 561
[20] de C Chamon C, Mudry C and Wen X-G 1996 *Phys. Rev.* B **53** R7638
Mudry C, de C Chamon C and Wen X-G 1996 *Nucl. Phys.* B **466** 383
de C Chamon C, Mudry C and Wen X-G 1996 *Phys. Rev. Lett.* **77** 4194
Castillo H E, de C Chamon C, Fradkin E, Goldbart P M and Mudry C 1997 *Phys. Rev.* B **56** 10668
[21] Altland A, Simons B D and Zirnbauer M R 2002 *Phys. Rep.* **359** 283
[22] Dyson F J 1953 *Phys. Rev.* **92** 1331
[23] Anderson P W 1958 *Phys. Rev.* **109** 1498
[24] Motrunich O, Damle K and Huse D A 2002 *Phys. Rev.* B **65** 064206
Motrunich O, Damle K and Huse D A 2001 *Phys. Rev.* B **63** 224204
[25] Guruswamy S, Le Clair A and Ludwig A W W 2000 *Nucl. Phys.* B **583** 475
[26] Mudry C, Ryu S and Furusaki A 2002 *Preprint* cond-mat/0207723
[27] Ryu S and Hatsugai Y 2002 *Phys. Rev.* B **65** 033301 and references therein
[28] Hatsugai Y, Wen X-G and Kohmoto M 1997 *Phys. Rev.* B **56** 1061
[29] Denteneer P J H, Scalettar R T and Trivedi N 2001 *Phys. Rev. Lett.* **87** 146401
[30] Abrahams E, Kravchenko S V and Sarachik M P 2001 *Rev. Mod. Phys.* **73** 251
[31] Evangelou S N 1986 *J. Phys. C: Solid State Phys.* **19** 4291
Evangelou S N 1990 *J. Phys: Condens. Matter* **2** 2953
[32] Grzonka R P and Moore M A 1982 *J. Phys. C: Solid State Phys.* **15** 5393
[33] Miller J and Wang J 1996 *Phys. Rev. Lett.* **76** 1461
[34] Oppermann R and Wegner F J 1979 *Z. Phys.* B **34** 327
[35] Cerovski V Z 2000 *Phys. Rev.* B **62** 12775
Cerovski V Z 2001 *Phys. Rev.* B **64** 161101
[36] Falko V I and Efetov K B 1995 *Phys. Rev.* B **52** 17413
[37] Ziman T A L 1982 *Phys. Rev.* B **26** 7066
[38] Paige C C 1972 *J. Inst. Math. Applic.* **10** 373
Paige C C 1976 *J. Inst. Math. Applic.* **18** 341
Parlett B N *The Symmetric Eigenvalue Problem* (Englewood Cliffs, NJ: Prentice-Hall)
[39] Shepelyansky D 1994 *Phys. Rev. Lett.* **73** 2607–10
[40] De Toro Arias S, Waintal X and Pichard J-L 1998 *Eur. Phys. J.* B **10** 149
[41] Mosseri R 2000 *J. Phys. A: Math. Gen.* **33** L319
[42] Hui V C and Lambert C J 1993 *J. Phys. C: Condens. Matter* **5** 697
Lambert C J and Hui V C 1990 *J. Phys. C: Condens. Matter* **2** 7303
[43] Katsanos D E, Evangelou S N and Lambert C J 1988 *Phys. Rev.* B **58** 2442
[44] Steiner M, Chen Yang, Fabricio M and Gogolin A O 1999 *Phys. Rev.* B **59** 14848
[45] Fabrizio M and Castellani C 2000 *Nucl. Phys.* B **583** 542